

# Investigating Splicing Variants Uncovered by Next-Generation Sequencing the Alzheimer's Disease Candidate Genes, *CLU*, *PICALM*, *CR1*, *ABCA7*, *BIN1*, the *MS4A* Locus, *CD2AP*, *EPHA1* and *CD33*

Naomi Clement<sup>1\*</sup>, Anne Braae<sup>1\*</sup>, James Turton<sup>1</sup>, Jenny Lord<sup>1</sup>, Tamar Guetta-Baranes<sup>1</sup>, Christopher Medway<sup>1</sup>, Keeley J Brookes<sup>1</sup>, Imelda Barber<sup>1</sup>, Tulsi Patel<sup>1</sup>, Lucy Milla<sup>1</sup>, Maria Azzopardi<sup>1</sup>, James Lowe<sup>2</sup>, David Mann<sup>3</sup>, Stuart Pickering-Brown<sup>3</sup>, Noor Kalsheker<sup>1</sup>, Peter Passmore<sup>4</sup>, Sally Chappell<sup>1\*</sup> and Kevin Morgan<sup>1\*</sup>; Alzheimer's Research UK (ARUK) Consortium<sup>†</sup>

<sup>1</sup>Human Genetics Group, School of Life Sciences, Queens Medical Centre, University of Nottingham, Nottingham, UK

<sup>2</sup>Neuropathology, School of Medicine, Queens Medical Centre, University of Nottingham, Nottingham, UK

<sup>3</sup>Clinical Neuroscience Research Group, Greater Manchester Neurosciences Centre, University of Manchester, Salford, UK

<sup>4</sup>Centre for Public Health, School of Medicine, Dentistry, and Biomedical Sciences, Queen's University Belfast, Belfast, Northern Ireland, UK

<sup>†</sup>The Alzheimer's Research UK (ARUK) Consortium comprises Peter Passmore, David Craig, Janet Johnston, Bernadette McGuinness, Stephen Todd, Queen's University Belfast, UK; Reinhard Heun, Royal Derby Hospital, UK; Heike Kölsch, University of Bonn, Germany; Patrick G. Kehoe, University of Bristol, UK; Emma R.L.C. Vardy, University of Salford, UK; Nigel M. Hooper, Stuart Pickering-Brown, University of Manchester, UK; Julie Snowden, Anna Richardson, Matt Jones, David Neary, Jenny Harris, Salford Royal NHS Foundation Trust, UK & University of Manchester, UK; Keeley Brookes, Christopher Medway, James Lowe, Kevin Morgan, University of Nottingham, UK; A. David Smith, Gordon Wilcock, Donald Warden, University of Oxford (OPTIMA), UK; Clive Holmes, University of Southampton, UK

\*Equal contribution

## Abstract

Late onset Alzheimer's disease (LOAD), the most common cause of late onset dementia, has a strong genetic component. To date, 21 disease-risk loci have been identified through genome wide association studies (GWAS). However, the causative functional variant(s) within these loci are yet to be discovered. This study aimed to identify potential functional splicing mutations in the nine original GWAS-risk genes: *CLU*, *PICALM*, *CR1*, *ABCA7*, *BIN1*, the *MS4A* locus, *CD2AP*, *EPHA1* and *CD33*. Target enriched next generation sequencing (NGS) was used to resequence the entire genetic region for each of these GWAS-risk loci in 96 LOAD patients and *in silico* databases were used to annotate the variants for functionality. Predicted splicing variants were further functionally characterised using splicing prediction software and minigene splicing assays. Following *in silico* annotation, 21 variants were predicted to influence splicing and, upon further annotation, four of these were examined utilising the *in vitro* minigene assay. Two variants, rs881768 A>G in *ABCA7* and a novel variant 11: 60179827 T>G in *MS4A6A* were shown, in these cell assays, to affect the splicing of these genes. The method employed in the paper successfully identified potential splicing variants in GWAS-risk genes. Further investigation will be needed to understand the full effect of these variants on LOAD risk. However, these results suggest a possible pipeline in order to identify putative functional variants as a result of NGS in disease-associated loci although improvements are needed within the current prediction programme in order to reduce the number of false positives.

**Keywords:** Late onset Alzheimer's disease; Next generation sequencing; Splicing; Annotation; Functional variations; Minigene assays

## Introduction

Late onset Alzheimer's disease (LOAD) is an insidious neurodegenerative disease responsible for most cases of dementia in the elderly. Despite being widely studied, the disease still lacks a clear pathogenesis. However, there is a strong genetic component to LOAD with 21 disease-risk genetic regions having been identified through genome wide association studies (GWAS) [1]. Due to the nature of GWAS experimental design, the variants associated through GWAS are frequently not the causal functional variants generating the disease association. Instead, one or several variants in linkage disequilibrium (LD) with the GWAS variant are likely to be causal [2,3]. Therefore, due to the large number of the possible causative functional variants within these loci, the mechanistic role that each of the identified 21 disease-risk genes may play in the progression of LOAD remains unknown.

To identify the disease-causing functional variant(s), a number of next-generation sequencing (NGS) studies have been undertaken for the LOAD GWAS loci. Examples include *CLU* [4], *CLU*, *PICALM* and *CR1* [5], *ABCA7* [6] and *ABCA7*, *BIN1*, *CD2AP*, *CLU*, *CR1*, *EPHA1*, *MS4A4/MS4A6A* [7]. All studies, apart from [5], have used targeted exome sequencing, ignoring variants which may be found in the

noncoding and intronic regions of the loci. Exome sequencing may also miss exonic variants which are found close to exon/intron borders [8]. Therefore these studies may have overlooked mutations which could affect splicing through disrupting donor and acceptor splice sites.

Splicing plays an important role in human genetic disease. Almost a third of currently known disease-causing variants disrupt splicing, although this is likely to be an underestimate [9,10]. Aberrant splicing is implicated in many neurodegenerative disorders [11] and in LOAD, variants causing dysfunctional splicing have been found in some of the risk genes including *PICALM* and *CD33* [12-14].

**\*Corresponding author:** Kevin Morgan, Human Genetics, School of Life Sciences, A Floor, West Block, Room 1306, Queens Medical Centre, University of Nottingham, Nottingham, NG7 2UH, United Kingdom, Tel: +44 115 8230724; E-mail: [Kevin.Morgan@nottingham.ac.uk](mailto:Kevin.Morgan@nottingham.ac.uk)

**Received** October 03, 2016; **Accepted** October 22, 2016; **Published** October 29, 2016

**Citation:** Clement N, Braae A, Turton J, Lord J, Guetta-Baranes T, et al. (2016) Investigating Splicing Variants Uncovered by Next-Generation Sequencing the Alzheimer's Disease Candidate Genes, *CLU*, *PICALM*, *CR1*, *ABCA7*, *BIN1*, the *MS4A* Locus, *CD2AP*, *EPHA1* and *CD33*. J Alzheimers Dis Parkinsonism 6: 276. doi: 10.4172/2161-0460.1000276

**Copyright:** © 2016 Clement N, et al. This is an open-access article distributed under the terms of the Creative Commons Attribution License, which permits unrestricted use, distribution, and reproduction in any medium, provided the original author and source are credited.

The aim of this study was to discover potentially functional causative splicing variants in the original nine genes highlighted through GWAS in 2009: *CLU*, *PICALM* [15], *CR1* [16], *ABCA7*, *BIN1*, the *MS4A* locus, *CD2AP*, *EPHA1* and *CD33* [17]. Target enrichment and next generation sequencing (NGS) were used to sequence the entire GWAS locus for each gene as identified through linkage disequilibrium. Coding and non-coding variants were prioritised for causality using functional annotation. Many of the variants were located close to intron/exon boundaries, suggesting a possible role in splicing. These variants were taken forward for further *in silico* investigation and experimental assessment of functionality.

## Methods

### NGS

Informed consent was obtained from all participants and the local Ethics Committee approved the study. 96 CERAD post-mortem confirmed LOAD brain tissue samples were obtained from the University of Nottingham Brain Bank (n=50) and the Manchester Brain Bank (n=46). This sample size gave 80% power to detect variants with a minor allele frequency (MAF) as low as 0.85% at a particular location. All samples were Caucasian, 52.8% female, with average age at onset of 70.8 years and *APOE* alleles:  $\epsilon$ 2-9.1%;  $\epsilon$ 3-57.2%;  $\epsilon$ 4-33.7%, data taken when consent obtained or upon receipt of the biological samples. DNA was extracted using phenol chloroform, quantified using Quant-iT™ ds DNA Broad Range Assay kit (Invitrogen) and combined into eight equimolar pools of 12 for a total concentration of 6 ug per pool (500 ng per sample).

Agilent SureSelect Custom MP3 kit designed on eArray with 5X tiling was used for target enrichment of LOAD associated genes including introns, exons and flanking conserved sequence. For *ABCA7*, *BIN1*, *CD33*, *CR1*, *CD2AP*, *EPHA1* and the *MS4A* locus, repetitive elements were masked in SureSelect bait design and the enriched library was sequenced by Source BioScience using 100 bp paired-end sequencing on the Illumina HiSeq 2000 and base called with Illumina Casava 1.9. SureSelect baits for *PICALM* and *CLU* were not repeat masked and were sequenced separately on the Illumina GAIIX with 38 bp single-end reads separately. Genomic regions potentially captured by these baiting strategies, as well as the transcript IDs for each of the genes used, are shown in (Table 1).

Raw data was quality control (QC) checked by FastQC prior to alignment to hg19 with BEAST v0.7.0a [18], following the program's protocol for the read type. Aligned files were manipulated using SAMtools v0.1.18 [19] and the success of the alignment was assessed with SAMtools flagstat function and SAMstat [20]. Variants were called

using the pooled data specific program, CRISP [21]. Called variants were filtered following the best practice variant detection suggested by Genome Analysis ToolKit pipeline (GATK v4.0, Broad Institute [22]). Variants were annotated using Ensembl's Variant Effect Predictor (VEP) [23] supplemented with annotations from Encyclopaedia of DNA Elements (ENCODE) project and PhastCons downloaded from the UCSC genome browser website (<http://genome.ucsc.edu/ENCODE/downloads.html>, accessed Nov 2012 [24]) using a custom in-house script. 21 variants identified as potentially affecting splicing (falling within 1-3 bp of exon and 1-12 bp of intron) were carried forward for further investigation. Given the difficulties identifying intronic mutations which affect branch point sites and the large number of intronic variants called, these were not taken forward in this project. Linkage disequilibrium (LD) between the variants of interest and the GWAS variants were calculated with VCFtools [25] using 1000Genomes Phase 1 data for samples of northern European Ancestry [26].

### *In silico* analysis of splicing

Additional *in silico* programs were used to assess the 21 identified splicing SNPs. Namely, ESEfinder v3 ([http://rulai.cshl.edu/cgi-bin/tools/ESE3/ese\\_finder.cgi?process=home](http://rulai.cshl.edu/cgi-bin/tools/ESE3/ese_finder.cgi?process=home)) [27], Berkley Drosophila Genome Project Splice Site Prediction by Neural Network (BDGP) ([http://www.fruitfly.org/seq\\_tools/splice.html](http://www.fruitfly.org/seq_tools/splice.html)) [28] and Human Splicing Finder (HSF) (<http://www.umd.be/HSF3/>) [29]. All programs were accessed March 2015.

Four potential variants were taken forward that showed differences between the two alleles in all three programs, including a score change of more than 10% between the major and the alternative allele where numerical scores were provided.

### *In vitro* analysis of splicing

As additional brain tissue was not available for all samples in order to perform RNA extractions, as well as the previous DNA extractions already performed, the minigene assay was selected to validate potential splicing variants. This method has been shown to have complete concordance with RT-PCR analysis of patient RNA and is a validated and reliable method for investigating splicing [30].

All methods were performed following manufacturer's protocol unless otherwise specified. The specific sample in each pool containing the heterozygous splice variant was identified by Sanger sequencing the appropriate exon(s) in each locus.

Minigene primers with the addition of *Sall* and *XbaI* restriction enzyme binding sites were designed using the relevant *ABCA7*, *MS4A6A* and *EPHA1* reference sequences using Primer 3 (v.0.4.0)

Gene	Transcript ID	Chromosome	Coordinates	BP
<i>CLU</i>	NM_001831.3	8	27 450 849-27 475 277	24,430
<i>PICALM</i>	NM_007166.3	11	85 665 237-85 783 519	118,280
<i>CR1</i>	NM_000651	1	207 667 495-207 816 719	149,224
<i>ABCA7</i>	NM_019112	19	1 038 952-1 066 720	27,768
<i>BIN1</i>	NM_139343.2	2	127 778 085-127 895 723	117,638
<i>MS4A LD Locus</i>	NG_016014	11	59 856 028-60 041 296	185,268
	NM_152852			
	XM_005274415			
<i>CD2AP</i>	NM_012120	6	47 427 281-47 601 015	173,734
<i>EPHA1</i>	NM_005232	7	143 082 382-143 110 385	28,003
<i>CD33</i>	NM_001772	19	51 718 317-51 748 546	30,229

**Table 1:** Regions of the genome (chromosome number and coordinates) to be targeted by Agilent SureSelect baits for the sequencing project. Coordinates are given relative to hg19. BP refers to how many bases can potentially be covered by the design. The Ensembl transcript IDs presented were utilised in all analysis of the sequence data as well as annotation of variants

(<http://frodo.wi.mit.edu/primer3/>). Amplicons were designed to contain the potential splicing mutations, adjacent exons and intronic sequences (Supplementary Table 1).

Initial PCR was carried out using 10-100 ng template DNA in 30 µl reaction volumes with Expand High Fidelity Taq (Roche). PCR conditions for all reactions were as follows: an initial denaturing step of 2 min at 94°C, followed by 30 cycles of 15 s at 94°C, 30 s at optimized annealing temperature ( $T_a$ , Supplementary Table 1) and 40 s, plus 5 s every cycle, at 72°C with a final extension step at 72°C for 7 min.

Amplicons were cloned into pCR 2.1-TOPO vectors using the TOPO TA Cloning kit (Invitrogen, Life Technologies) before being ligated into the exon trap vector, pET01 (MoBiTech) and transformed into NEB High Efficiency 5-alpha chemically competent *E. coli* cells C2987I. Vector DNA was then extracted following the NucleoBond Xtra Midi Plus EF Kit in an endotoxin free environment as well as being sequenced to confirm the insert sequence was accurately cloned.

Two cell lines were obtained from the European Collection of Cell Cultures (ECCC): CV-1 in Origin, carrying SV40 (COS-7) derived from monkey African green kidney cells and human Caucasian neuroblastoma cells (BE(2)-C). COS-7 is typically used for testing minigene splicing assays as it is easy to transfect and grow, as well as being known to accurately represent the complex eukaryotic splicing environment seen *in vivo*. BE(2)-C cells were selected in order to investigate possible neurological-specific splicing effects due to the brain's unique spliceosome. COS-7 were cultured in Dulbecco's Modified Eagle Medium (DMEM) with 10% Foetal Bovine Serum (FBS), 2 mM L-Glutamine, 100 U/ml penicillin-streptomycin and 100 U/ml fungizone and BE(2)-C were cultured in 1:1 Eagle's Minimal Essential Medium (EMEM):Ham's F12 with 1% non-essential amino acids, 2 mM Glutamine, 15% FBS, 100 U/ml penicillin-streptomycin and 100 U/ml fungizone. The COS-7 and BE(2) cells were plated out at  $3.5 \times 10^5$  cells per plate and  $6 \times 10^5$  cells per plate, respectively. Cells were transfected using TransFact (Promega) and incubated for 24 h. The transfection was repeated in triplicate in each cell line. Total RNA was then extracted utilising the RNeasy Mini Kit (Qiagen) with the additional on column DNase treatment (TURBO DNA-free Kit, Ambion). Total cDNA was synthesised with AffinityScript Multiple Temperature cDNA Synthesis kit (Agilent) using oligodT primers. The cDNA of interest was then PCR amplified in a 30 µl reaction volume using LongAmp Taq (New England BioLabs) and primers specific to the pET01 vector (Forward: GATCGATCCGCTTCCTG, Reverse: CACTGGAGGTGGCCCCG). The thermal cycling conditions were: 30 s at 94°C for initial denaturation, followed by 30 cycles of 15 s at 94°C for denaturation, 30 s at 59°C for annealing and 50 s at 65°C for extension and 10 m at 65°C for the final extension. Amplicons were compared by electrophoresis as well as Sanger sequenced in order to undertake a more detailed comparison.

## Results

### NGS study

An average of 245.5 million reads per pool was obtained. The eight pools of twelve passed all FastQC parameters apart from sequence duplication which is to be expected given the sequencing strategy employed.

The flagstat analysis in SAMtools showed that 99% of reads were mapped correctly and 95-99% of reads were properly paired. CRISP called 3205 variants within the nine loci, with 760 novel variants. The minor allele frequency estimates from CRISP were strongly

positively correlated with frequencies found in the 1000 Genomes project indicating successful variant calling (Spearman Correlation Coefficient=0.60,  $p < 0.0001$  across all gene regions examined). Following annotation, only 126 exonic variants were called with the majority of variants being non-coding. There were 43 variants in untranslated regions (UTRs) and 44 missense variants (Supplementary Table 2). As defined above, 21 variants were predicted to affect splicing (Supplementary Table 2).

### *In silico* analysis of splicing

All 21 variants were further annotated by three *in silico* programs, the results of which can be seen in (Supplementary Table 3). From this original list of 21 variants, four were predicted to be splice site variants by at least two programs by altering the donor or acceptor sites (predicted by the BDGP and HSF programs) as well as altering splicing factor binding sites (predicted by ESEfinder) (Table 2). These variants (19:1054696 and rs881768 in *ABCA7*, 11:60179827 in *MS4A6A* and rs6967117 in *EPHA1*) were therefore analysed *in vitro* in order to assess the accuracy of these predictions.

### *In vitro* analysis of splicing

For two of the variants analysed (19:1054696 in *ABCA7* and rs6967117 in *EPHA1*) there was no difference between the RNA extracted from cells transfected with the wild-type insert and the mutant insert in both BE(2)-C and COS-7 cell lines. This was apparent on both gel electrophoresis and sequencing of the RT-PCR products.

The *ABCA7* variant rs881768 A>G, however, produced different results between the wild-type and mutant constructs upon analysis of RT-PCR products, as shown in (Figure 1). The major product with both constructs (when either the A or G allele was present) had exon 32 spliced out, leaving only vector sequence. With the mutant construct there was also a minor product, where exon 32 was included, suggesting low levels of exon 32 inclusion with the minor allele haplotype. This was evident in both COS-7 and BE(2)-C cell lines.

The *MS4A6A* variant at genomic position 11: 60179827 T>G also showed some differences between constructs, presented in (Figure 2). The major product with the wild-type construct, as predicted, contained both the vector exons and exon 4 of the gene. There was also a minor product present which contained just the vector sequence, suggesting low levels of a gene product with this exon spliced out. The only product with the mutant construct showed exon 4 spliced out. These results were obtained with both COS-7 and BE(2)-C cells lines.

## Discussion

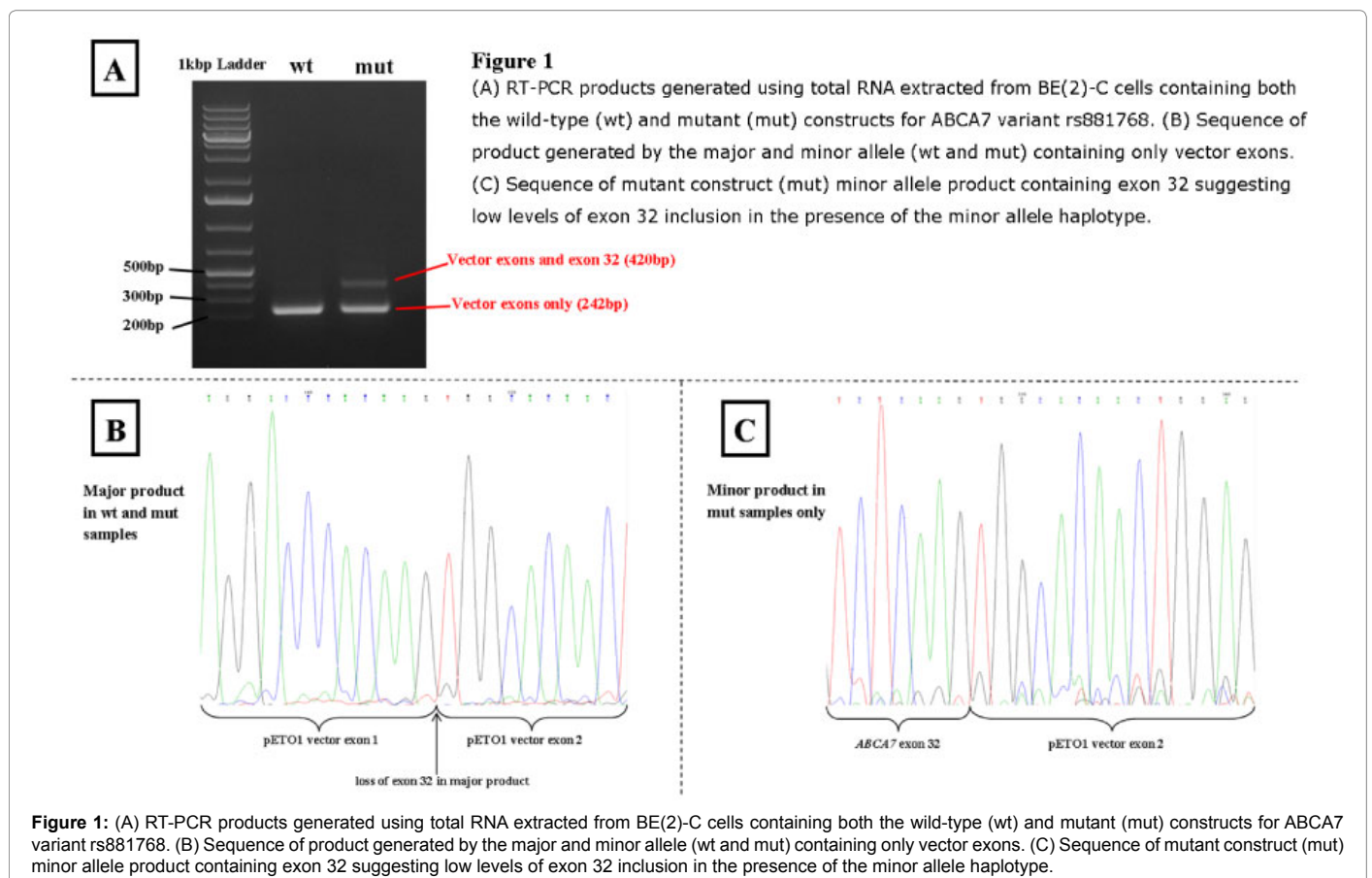
A 2013 GWAS meta-analysis for LOAD used over 74000 samples to identify 11 new disease-risk genes and confirmed 10 previous susceptibility loci (*CLU*, *PICALM*, *CR1*, *BIN1*, *ABCA7*, the *MS4A* locus, *CD2AP*, *EPHA1*, the *HLA-DRB5-HLA-DRB1* locus, *PTK2B*, *SORL1*, *SLC24A4-RIN3*, *INPP5D*, *MEF2C*, *NME8*, *ZCWPW1*, *CELF1*, *FERMT2* and *CASS4* [1]). The population attributable risk for each of these loci range from 1 to 8% indicating further genetic risk factors remain to be discovered for LOAD [1].

This study used targeted sequencing to identify 21 potential splicing variants located in nine of the original genetic loci associated with LOAD in 96 patients. Following the *in silico* assessment of the variants' impact on splicing, four variants were put forward for *in vitro* confirmation using hybrid minigenes in the pET01 vector. Only two of the variants were confirmed to be functional; rs881768 A>G in *ABCA7* and novel variant 11: 60179827 T>G in *MS4A6A*, part of the

Gene (Transcript ID)	Genomic Location (rsID)	Transcript location	Ref/Alt	MAF	D'	ESEfinder	BDGP	Human Splicing Finder	Combined predicted consequence
<b>ABCA7</b> (NM_019112)	19:1054696 (-)	Intron 28-29 +3 bp	G/C	0.010	NA	SRSF2 site gained	Known functional donor site with a score of 0.91 reduced to a score of 0.38	Alteration of an intronic ESS site.	Change in ESE and intronic ESS site could change transcript isoform ratio.
	19:1056066 (rs881768)	Exon 32 1 bp	A/G	0.250	-0.824	SRSF1 site gained, SRSF6 site lost	Novel donor site created with a score of 0.98 Strengthens known functional acceptor site score from 0.56 to 0.76	A cryptic donor site is activated.	Activation of donor site at start of exon might result in exon skipping.
<b>MS4A6A*</b> (NM_152852)	11: 60179827 (-)	Intron 4-5 +4 bp	T/G	0.480	NA	SRSF5 sites lost	Known functional donor site with a score of 0.66 lost	Activation of intronic cryptic acceptor site, and intronic cryptic donor site and creation of intronic ESE site.	Loss of existing donor site could result in exon skipping. However, activating intronic acceptor or donor site could result in a change in the sequence included in the exon.
<b>EPHA1*</b> (NM_005232)	7:143391774 (rs6967117)	Exon 17 +1bp	T/C	0.060	0.75	SRSF1 site gained	Novel donor site created with score of 0.49.	A cryptic donor site is activated.	Activation of donor site at start of exon might result in exon skipping.

**Table 2:** Prioritised splicing variants from the NGS study selected for further experimental investigation.

Genomic location is relative to GRCh38 and rsID is provided where available, (-) defines no rsID for this genomic location. Genes located on the reverse strand are indicated (\*) and transcripts of these genes used are provided, defined by Ensembl.org. The reference and alternative allele for the forward strand as called in CRISP are shown (Ref/Alt) as is the minor allele frequency (MAF). The Linkage Disequilibrium between the SNP presented and the GWAS tag SNP for that gene is also presented in the D' format. "NA" defines the LD is unavailable, most likely due to the variant in question not being present in the CEU population in the 1000 Genomes database. All variants resulted in results indicating they have the potential to alter splicing by all three *in silico* programmes used (ESEfinder, BDGP and Human Splicing Finder). SRSF = Serine/arginine-rich splicing factor, ESE=Exonic Splicing Enhancer and ESS=Exonic Splicing Suppressor.



*MS4A* locus. This suggests that the methods currently used to prioritize potential functional variants need further refinement.

The synonymous variant rs881768 is located at the first base of exon 32 in *ABCA7* (transcript ID NM\_019112) and is in linkage disequilibrium with the *ABCA7* GWAS variant (D'=0.824, Table 2). *In*

*silico* predictions suggest that the G allele creates a new donor site with a similar score to the original donor site, located only 126 bp away (a score of 0.98 compared with 0.99) and changes the binding of two exon splicing enhancer (ESE) proteins (Table 2). These predictions suggest the G allele could activate a cryptic splice site or cause a change in protein isoform ratios. However, population data from 1000 Genomes

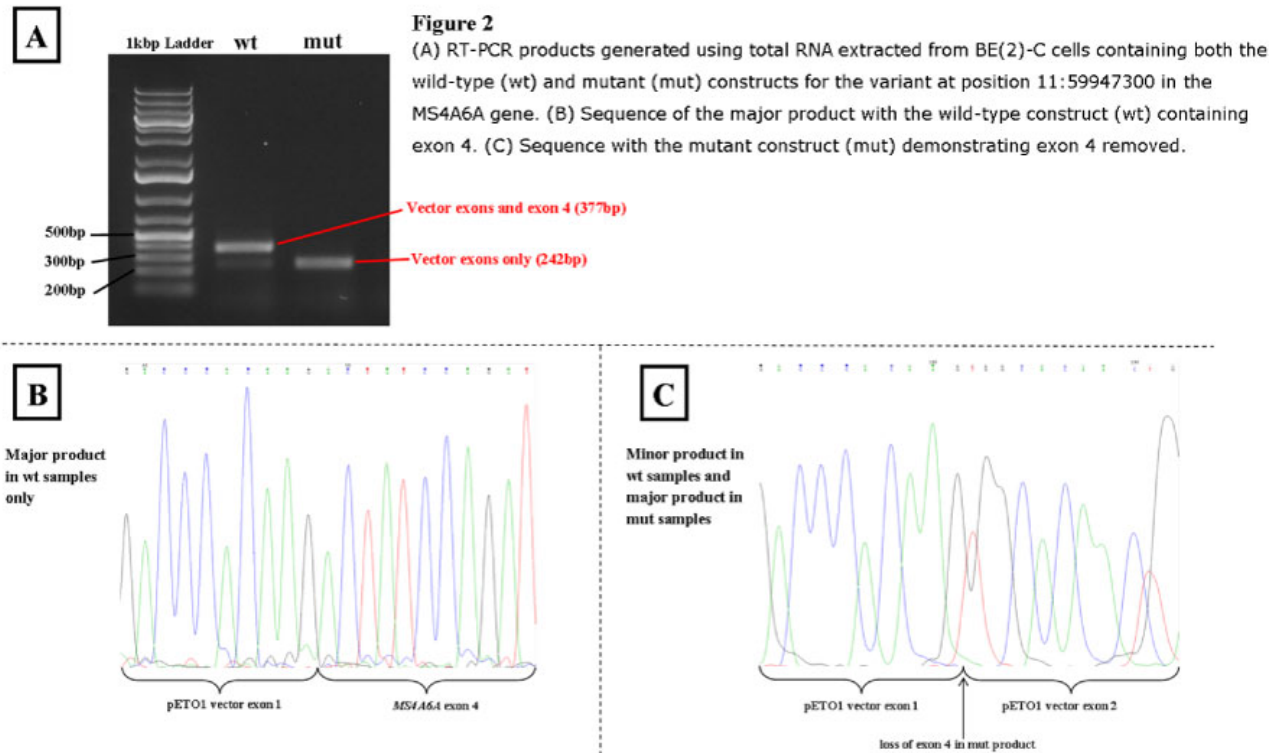


**Figure 2:** (A) RT-PCR products generated using total RNA extracted from BE(2)-C cells containing both the wild-type (wt) and mutant (mut) constructs for the variant at position 11:59947300 in the *MS4A6A* gene. (B) Sequence of the major product with the wild-type construct (wt) containing exon 4. (C) Sequence with the mutant construct (mut) demonstrating exon 4 removed.

shows that the G allele is actually the ancestral allele with a European population allele frequency of 0.44. Additionally, score predictions for the acceptor site shows that the A allele has a lower score than the G allele (0.56 compared to 0.76) which could lead to exon skipping. This makes *in silico* functional prediction of this variant very difficult.

In the minigene assays the G allele causes low levels of exon 32 to be incorporated into the transcript, while the A allele causes exon 32 to be spliced out. Expressed sequence tag (EST) databases such as GTEX portal [31] show exon 32 is incorporated in most transcripts and utilising this transcript data to examine the effect of rs881768 shows that this variant has no effect on splicing in this database. *ABCA7* has an interesting pattern of alternative splicing, with many introns consisting of multiples of three, potentially allowing in-frame addition and deletion of introns, although no such transcripts have been identified. Exon 32, however, does result in a frame-shift change creating a termination codon in the next exon and causing early truncation of the protein. This truncated protein is non-functional as it lacks the last five transmembrane domains and the second nucleotide binding domain and may be targeted for nonsense mediated decay. This would prevent any truncated proteins being expressed causing sole expression of the complete isoform, explaining the lack of this truncated protein in databases such as GTEX.

The novel variant identified in *MS4A6A*, part of the *MS4A* locus, 11:60179827 T>G is found 4 bp into the intron between exon 4 and 5. The G allele removes the native donor site for exon 4/intron 4 possibly causing exon skipping (Table 2). However, a cryptic donor site is activated and the binding of two ESE proteins are affected, potentially changing the sequence included in the transcript. The minigene assays show that the G allele does appear to cause exon skipping, creating

transcripts without exon 4. However, the T allele, while mostly producing transcripts which contain exon 4, also produces a small proportion of transcripts without exon 4. Transcripts without exon 4 appear to be produced by both alleles despite the removal of exon 4 generating a truncated protein which lacks two transmembrane domains and one noncytoplasmic domain. Although the G allele does cause exon 4 to be excluded through obliterating the donor site, there must be additional alternative splicing regulation mechanisms occurring within the *in vitro* assay, as well as *in vivo*, which affect the levels of each isoform being produced explaining the presence of both isoforms in the presence of the T allele.

To fully explore the role both of these variants play in splicing, direct analysis of RNA samples from affected tissues from LOAD individuals with the variants should be examined. Unfortunately for rare variants in LOAD this tissue is not always readily available. Epstein-Barr transformed cell lines used for 1000 Genomes project, however, are a possible alternative. Targeted sequencing of RNA extracted from these cell lines selected to be homozygous for different alleles could be compared to the results of the minigene assays. This would determine the role of these splicing variants in an environment where the whole genome is present, rather than just the fragment inserted in the minigene assay. There is also publicly available RNA-seq data from these cell lines (see the GEUVADIS project [32]); unfortunately coverage for many of the LOAD risk loci is poor.

While only two variants show aberrant splicing in this study, dysfunctional splicing has been previously implicated in LOAD. Distinctive patterns of alternative splicing and promoter use were discovered in LOAD brain tissue through comparing the transcriptome profiles of the frontal, temporal and parietal lobes of AD patients with

controls [33,34]. Additionally, small nuclear and heterogeneous nuclear ribonucleoproteins have been shown to be disrupted in LOAD [35,36]. Therefore the role of splicing in LOAD disease pathology should not be ignored.

Identifying variants that have a functional role in complex diseases is a challenge [37]. This is particularly true for next generation sequencing studies which identify large numbers of potential functional variants. The problem arises while attempting to prioritise the variants for further functional assays or experiments. Current *in silico* databases have minimal experimental information available. The annotation programs used need to be chosen carefully in order to correctly assign potential functionality and ensure pathogenic variants are found.

Prediction algorithms for exonic and intronic splicing enhancer and silencer sites are less robust than programs predicting disruptions of 3' and 5' consensus splice site regions. This is largely because more is known about the 3' acceptor and 5' donor consensus sequences, thus allowing better prediction models to be built [38]. Due to this, the initial selection of splicing variants in this study selected variants within 1-3 bp of an exon or 1-12 bp of an intron, biasing the selection towards variants that may disrupt consensus splice sites. The BDGP and HSF prediction programs used in this study both examine the effects of mutations on 3' (acceptor) and 5' (donor) consensus sequences. The two variants that had an effect on splicing *in vitro* were both predicted to affect acceptor and/or donor consensus sites by BDGP and HSF (Table 2).

The recognition of exon and intron borders in pre-mRNA by the spliceosome does not simply involve identifying the correct consensus 3' and 5' splicing sequences. A multitude of splicing regulatory proteins and ribonucleoproteins interact to precisely control splicing and influence the levels of different transcript isoforms created [39]. Many variants that disrupt splicing are found deep within exons and introns and affect splicing through the disruption of exonic or intronic splicing enhancers or silencers [40]. Through limiting the analysis to variants located near consensus splice sites, as in this study, these mutations will be missed. With the advent of additional functional experimental studies, predictions of mutations influencing the binding of RNA proteins can only improve and would be useful for future work. This issue has recently been addressed by ANNOVAR, with the option to include bulk annotations from the SPIDEX dataset. This dataset provides an improved algorithm for detecting potential splicing variants [41]. However, a review of the method suggests that two other prediction methods for exonic splicing regulatory elements may perform better [42].

## Conclusion

Pooled NGS with target enrichment successfully identified potential functional splicing variants in nine gene regions associated with LOAD. Through targeting the entire genomic sequence, we were able to investigate variants in these regions which potentially affect consensus splice sites *in silico* and *in vitro*. Improvements are needed in current splicing prediction programs to reduce the number of false positives which are taken forward for analysis as well as reducing the number of false negatives discarded prior to further investigation. Further work is needed to fully clarify the role that the variants rs881768 (*ABCA7*) and 11: 60179827 T>G (*MS4A6A*) may have in LOAD *in vivo*.

## Acknowledgement

The Nottingham Group are funded by Alzheimer's Research UK and the Big Lottery Fund. NC was funded by a scholarship from The Jean Shanks Foundation. MA was funded by the MASTER it! Scholarship Scheme; this scholarship is part-financed by the European Union – European Social Fund.

## References

1. Lambert JC, Ibrahim-Verbaas CA, Harold D, Naj AC, Sims R, et al. (2013) Meta-analysis of 74,046 individuals identifies 11 new susceptibility loci for Alzheimer's disease. *Nat Genet* 45:1452-1458.
2. Schaub MA, Boyle AP, Kundaje A, Batzoglu S, Snyder M (2012) Linking disease associations with regulatory information in the human genome. *Genome Res* 22: 1748-1759.
3. Altshuler DM, Gibbs RA, Peltonen L, Dermitzakis E, Schaffner SF, et al. (2010) Integrating common and rare genetic variation in diverse human populations. *Nature* 467: 52-58.
4. Bettens K, Brouwers N, Engelborghs S, Lambert JC, Rogaeve E, et al. (2012) Both common variations and rare non-synonymous substitutions and small insertion/deletions in *CLU* are associated with increased Alzheimer risk. *Mol Neurodegener* 7: 3.
5. Lord J, Turton J, Medway C, Shi H, Brown K, et al. (2012) Next generation sequencing of *CLU*, *PICALM* and *CR1*: Pitfalls and potential solutions. *Int J Mol Epidemiol Genet* 3: 262-275.
6. Cuyvers E, De Roeck A, Van den Bossche T, Van Cauwenberghe C, Bettens K, et al. (2015) Mutations in *ABCA7* in a Belgian cohort of Alzheimer's disease patients: a targeted resequencing study. *Lancet Neurol* 14: 814-822.
7. Vardarajan BN, Ghani M, Kahn A, Sheikh S, Sato C, et al. (2015) Rare coding mutations identified by sequencing of Alzheimer disease genome-wide association studies loci. *Ann Neurol* 78: 487-498.
8. Belkadi A, Bolze A, Itan Y, Cobat A, Vincent QB, et al. (2015) Whole-genome sequencing is more powerful than whole-exome sequencing for detecting exome variants. *Proc Natl Acad Sci USA* 112: 5473-5478.
9. Lim KH, Ferraris L, Filloux ME, Raphael BJ, Fairbrother WG (2011) Using positional distribution to identify splicing elements and predict pre-mRNA processing defects in human genes. *Proc Natl Acad Sci USA* 108: 11093-11098.
10. Sterne-Weiler T, Howard J, Mort M, Cooper DN, Sanford JR (2011) Loss of exon identity is a common mechanism of human inherited disease. *Genome Res* 21: 1563-1571.
11. Mills JD, Janitz M (2012) Alternative splicing of mRNA in the molecular pathology of neurodegenerative diseases. *Neurobiol Aging* 33: 1012.e11–1012.e24.
12. Schnetz-Boutaud NC, Hoffman J, Coe JE, Murdock DG, Pericak-Vance MA, et al. (2012) Identification and confirmation of an exonic splicing enhancer variation in exon 5 of the Alzheimer disease associated *PICALM* gene. *Ann Hum Genet* 76: 448-453.
13. Malik M, Simpson JF, Parikh I, Wilfred BR, Fardo DW, et al. (2013) *CD33* Alzheimer's risk-altering polymorphism, *CD33* expression and exon 2 splicing. *J Neurosci Off J Soc Neurosci* 33: 13320-13325.
14. Raj T, Ryan KJ, Replogle JM, Chibnik LB, Rosenkrantz L, et al. (2014) *CD33*: Increased inclusion of exon 2 implicates the Ig V-set domain in Alzheimer's disease susceptibility. *Hum Mol Genet* 23: 2729-27336.
15. Harold D, Abraham R, Hollingworth P, Sims R, Gerrish A, et al. (2009) Genome-wide association study identifies variants at *CLU* and *PICALM* associated with Alzheimer's disease. *Nat Genet* 41: 1088-1093.
16. Lambert JC, Heath S, Even G, Campion D, Sleegers K, et al. (2009) Genome-wide association study identifies variants at *CLU* and *CR1* associated with Alzheimer's disease. *Nat Genet* 41: 1094-1099.
17. Naj AC, Jun G, Beecham GW, Wang LS, Vardarajan BN, et al. (2011) Common variants at *MS4A4/MS4A6E*, *CD2AP*, *CD33* and *EPHA1* are associated with late-onset Alzheimer's disease. *Nat Genet* 43: 436-441.
18. Homer N, Merriman B, Nelson SF (2009) BFAST: an alignment tool for large scale genome resequencing. *PLoS One* 4: e7767.
19. Li H, Handsaker B, Wysoker A, Fennell T, Ruan J, et al. (2009) The sequence alignment/map format and SAMtools. *Bioinforma Oxf Engl* 25: 2078-2079.
20. Lassmann T, Hayashizaki Y, Daub CO (2011) SAMStat: Monitoring biases in next generation sequencing data. *Bioinforma Oxf Engl* 27: 130-131.
21. Bansal V, Libiger O, Torkamani A, Schork NJ (2010) Statistical analysis strategies for association studies involving rare variants. *Nat Rev Genet* 11: 773-785.
22. McKenna A, Hanna M, Banks E, Sivachenko A, Cibulskis K, et al. (2010)

- The genome analysis toolkit: A MapReduce framework for analyzing next-generation DNA sequencing data. *Genome Res* 20: 1297-1303.
23. McLaren W, Pritchard B, Rios D, Chen Y, Flicek P, et al. (2010) Deriving the consequences of genomic variants with the Ensembl API and SNP effect predictor. *Bioinforma Oxf Engl* 26: 2069-2070.
  24. Consortium TEP (2011) A user's guide to the encyclopedia of DNA elements (ENCODE). *PLoS Biol* 9: e1001046.
  25. Danecek P, Auton A, Abecasis G, Albers CA, Banks E, et al. (2011) The variant call format and VCFtools. *Bioinforma Oxf Engl* 27: 2156-2158.
  26. Abecasis GR, Auton A, Brooks LD, DePristo MA, Durbin RM, et al. (2012) An integrated map of genetic variation from 1,092 human genomes. *Nature* 491: 56-65.
  27. Cartegni L, Wang J, Zhu Z, Zhang MQ, Krainer AR (2003) ESEfinder: A web resource to identify exonic splicing enhancers. *Nucleic Acids Res* 31: 3568-3571.
  28. Reese MG, Eeckman FH, Kulp D, Haussler D (1997) Improved splice site detection in genie. *J Comput Biol* 4: 311-323.
  29. Desmet FO, Hamroun D, Lalonde M, Collod-Bérout G, Claustres M, et al. (2009) Human splicing finder: An online bioinformatics tool to predict splicing signals. *Nucleic Acids Res* 37: e67.
  30. Steffensen AY, Dandanell M, Jønson L, Ejlersen B, Gerdes AM, et al. (2014) Functional characterization of BRCA1 gene variants by mini-gene splicing assay. *Eur J Hum Genet EJHG* 22: 1362-1368.
  31. Ardlie KG, Deluca DS, Segre A V, Sullivan TJ, Young TR, et al. (2015) The genotype-tissue expression (GTEx) pilot analysis: Multitissue gene regulation in humans. *Science* 348: 648-660.
  32. Lappalainen T, Sammeth M, Friedländer MR, Höfer PAC, Monlong J, et al. (2013) Transcriptome and genome sequencing uncovers functional variation in humans. *Nature* 501: 506-511.
  33. Twine NA, Janitz K, Wilkins MR, Janitz M (2011) Whole transcriptome sequencing reveals gene expression and splicing differences in brain regions affected by Alzheimer's disease. *PLoS One* 6: e16266.
  34. Mills JD, Nalpathamkalam T, Jacobs HIL, Janitz C, Merico D, et al. (2013) RNA-Seq analysis of the parietal cortex in Alzheimer's disease reveals alternatively spliced isoforms related to lipid metabolism. *Neurosci Lett* 536: 90-95.
  35. Bai B, Hales CM, Chen PC, Gozal Y, Dammer EB, et al. (2013) U1 small nuclear ribonucleoprotein complex and RNA splicing alterations in Alzheimer's disease. *Proc Natl Acad Sci USA* 110: 16562-16567.
  36. Berson A, Barbash S, Shaltiel G, Goll Y, Hanin G, et al. (2012) Cholinergic-associated loss of hnRNP-A/B in Alzheimer's disease impairs cortical splicing and cognitive function in mice. *EMBO Mol Med* 4: 730-742.
  37. MacArthur DG, Manolio TA, Dimmock DP, Rehm HL, Shendure J, et al. (2014) Guidelines for investigating causality of sequence variants in human disease. *Nature* 508: 469-476.
  38. Jian X, Boerwinkle E, Liu X (2014) *In silico* tools for splicing defect prediction: A survey from the viewpoint of end users. *Genet Med Off J Am Coll Med Genet* 16: 497-503.
  39. DeConti L, Baralle M, Buratti E (2013) Exon and intron definition in pre-mRNA splicing. *Wiley Interdiscip Rev RNA* 4: 49-60.
  40. Sterne-Weiler T, Sanford JR (2014) Exon identity crisis: Disease-causing mutations that disrupt the splicing code. *Genome Biol* 15: 201.
  41. Xiong HY, Alipanahi B, Lee LJ, Bretschneider H, Merico D, et al. (2015) The human splicing code reveals new insights into the genetic determinants of disease. *Science* 347: 1254806.
  42. Soukariéh O, Gaildrat P, Hamieh M, Drouet A, Baert-Desurmont S, et al. (2016) Exonic splicing mutations are more prevalent than currently estimated and can be predicted by using *in silico* tools. *PLoS Genet* 12: e1005756.